

# Computer modeling of rhegmatogenous retinal detachment

Jan O. Pralits

Department of Civil, Chemical and Environmental Engineering  
University of Genoa, Italy  
jan.pralits@unige.it

June 17, 2015

**The work presented has been carried out in collaboration with:**

- **Damiano Natali** DICCA, University of Genoa, Italy
- **Rodolfo Repetto** DICCA, University of Genoa, Italy
- **Jennifer Tweedy (Siggers)** Imperial College London, UK
- **Tom H. Williamson** Retina Surgery, London, UK

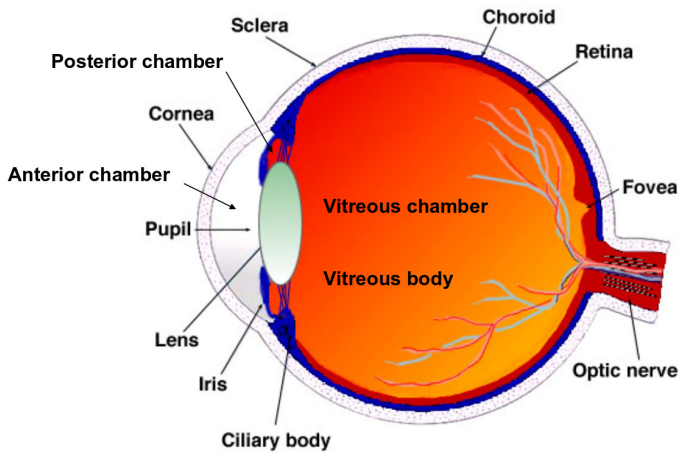
A paper is in preparation for *Investigative Ophthalmology & Visual Science (IOVS)*

**1 Introduction**

**2 Retinal break**

**3 References**

# Anatomy of the eye



# Anterior chamber I

## Flow mechanisms

### Flow induced by aqueous production/drainage:

Aqueous humor is produced by the ciliary body, and then flows through the posterior chamber, the pupil and the anterior chamber, from where it is drained into the trabecular meshwork. ( $3 \mu\text{l}/\text{min}$ )

### Flow induced during miosis/mydriasis:

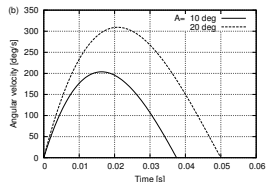
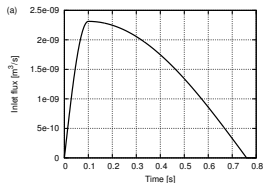
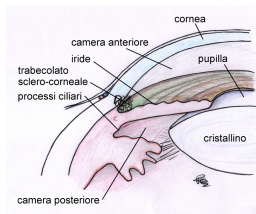
During pupil contraction (miosis), a flow from the posterior to the anterior chamber of the eye is generated, which is intense, although it only lasts a short time, typically less than 1 s. (**middle figure**)

### Buoyancy-driven flow:

It is well known that, since the posterior surface of the cornea is typically cooler than the iris and lens. We prescribed a temperature of  $34^\circ\text{C}$  on the cornea and  $37^\circ\text{C}$  on all other surfaces.

### Flow induced by saccades of the eye:

We consider the flow generated in the anterior chamber by rotations of the eye bulb by modeling isolated rotations using the analytical relationship proposed by Repetto et al. (2005) which provides the angular velocity of the eye as a function of time. (**bottom figure**)



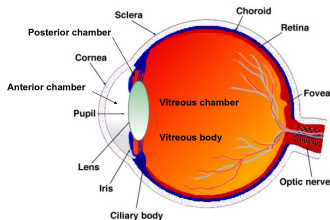
## Vitreous characteristics and functions

### Vitreous composition

The main constituents are

- Water (99%);
- hyaluronic acid (HA);
- collagen fibrils.

Its structure consists of long, thick, non-branching collagen fibrils suspended in hyaluronic acid.



### Normal vitreous characteristics

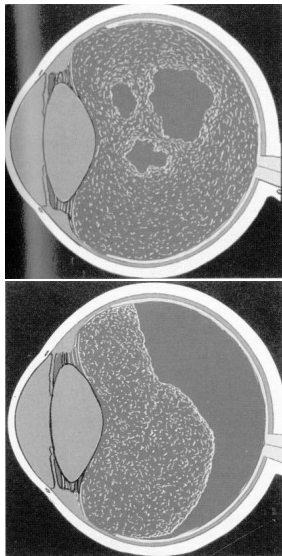
- The healthy vitreous in youth is a gel-like material with **visco-elastic mechanical properties**, which have been measured by several authors (Lee et al., 1992; Nickerson et al., 2008; Swindle et al., 2008).
- In the outermost part of the vitreous, named **vitreous cortex**, the concentration of collagen fibrils and HA is higher.
- The vitreous cortex is in contact with the **Internal Limiting Membrane (ILM)** of the retina.

### Physiological roles of the vitreous

- **Support function for the retina** and filling-up function for the vitreous body cavity;
- **diffusion barrier** between the anterior and posterior segment of the eye;
- establishment of an **unhindered path of light**.

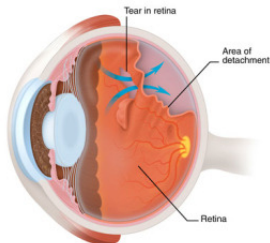
## Vitreous ageing

With advancing age the vitreous typically undergoes significant changes in structure.



- Disintegration of the gel structure which leads to **vitreous liquefaction (synchysis)**. This leads to an approximately linear increase in the volume of liquid vitreous with time. Liquefaction can be as much extended as to interest the whole vitreous chamber.
- Shrinking of the vitreous gel (**syneresis**) leading to the detachment of the gel vitreous from the retina in certain regions of the vitreous chamber. This process typically occurs in the posterior segment of the eye and is called **posterior vitreous detachment (PVD)**. It is a pathophysiologic condition of the vitreous.

# Retinal detachment



## Posterior vitreous detachment (PVD) and vitreous degeneration:

- more common in myopic eyes;
- preceded by changes in vitreous macromolecular structure and in vitreoretinal interface → possibly mechanical reasons.
- If the retina detaches from the underlying layers → loss of vision;

## Rhegmatogenous retinal detachment:

- fluid enters through a retinal break into the sub retinal space and peels off the retina.

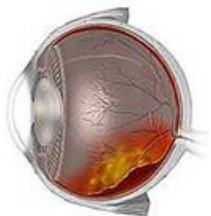
## Risk factors:

- **myopia**;
- posterior vitreous detachment (PVD);
- lattice degeneration;
- ...

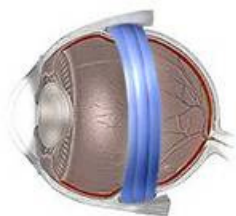
# Scleral buckling and vitrectomy

## Scleral buckling

Before



After



Scleral buckling is the application of a rubber band around the eyeball at the site of a retinal tear in order to promote reattachment of the retina.

## Vitrectomy



The vitreous may be completely replaced with tamponade fluids: silicon oils, water, gas, ..., usually immiscible with the eye's own aqueous humor

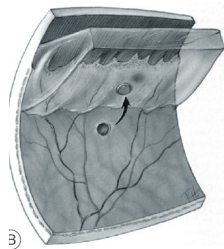
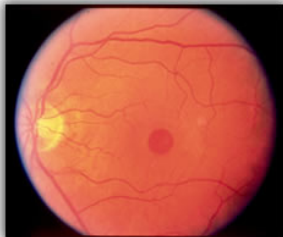
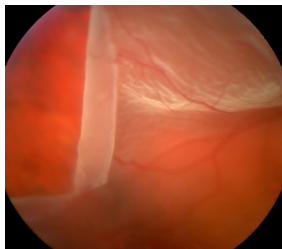
# Retinal break

## Rhegmatogenous retinal detachment

- Occurs in approximately **1 in 10,000** of the population.
- Caused by the appearance of retinal **breaks in the peripheral retina**
- Unchecked retinal detachment is a **blinding condition**
- There is uncertainty surrounding the mechanism of action of surgical methods.
- **Traction on the retina** from separation of the vitreous is thought to create the retinal break
- Postulated that **saccadic eye movements** create liquefied vitreous flow in the eye, which help to lift the retina.
- Experience says that the **hole** condition detaches quicker than the **free flap** condition

**Here:** use numerical simulations (**FSI**) to investigate the two cases under realistic conditions to give indications to surgeons.

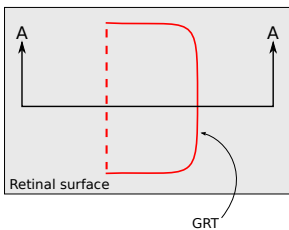
## The retinal detachment: cases considered here



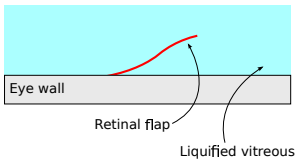
left) (GRT) Giant Retinal Tear (when large,  $>90^\circ$ ), middle) macular hole, right) retinal hole

# The retinal detachment: cases considered here

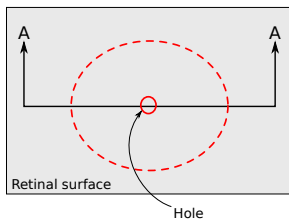
(a) Giant retinal tear



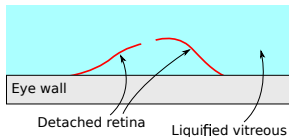
Section A-A



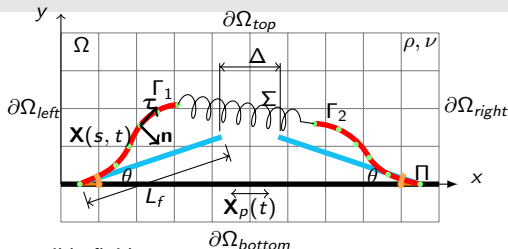
(b) Retinal hole



Section A-A



## Governing equations



For the viscous incompressible fluid

$$\begin{cases} \frac{\partial \mathbf{u}}{\partial t} + \mathbf{u} \cdot \nabla \mathbf{u} = -\nabla p + \frac{1}{Re} \nabla^2 \mathbf{u} + \mathbf{f} \\ \nabla \cdot \mathbf{u} = 0 \end{cases},$$

Periodicity is imposed at  $\partial\Omega_{left}$  and  $\partial\Omega_{right}$ , and symmetry at  $\partial\Omega_{top}$  and  $\partial\Omega_{bottom}$ . Non slip boundary conditions are imposed on solid surfaces.

For the slender 1D structure

$$\rho_1 \frac{\partial^2 \mathbf{X}}{\partial t^2} = \frac{\partial}{\partial s} \left( T \frac{\partial \mathbf{X}}{\partial s} \right) - \frac{\partial^2}{\partial s^2} \left( K_b \frac{\partial^2 \mathbf{X}}{\partial s^2} \right) + \rho_1 \mathbf{g} - \mathbf{F}$$

The structure is clamped at a certain angle  $\theta$  at the wall, which moves according to  $\mathbf{X}_p(t)$ . Incompressibility of the structure is imposed and non-slip/no penetration of the fluid is enforced.

## Dimensionless parameters

The governing equations can be non-dimensionalized with the following characteristic scales:

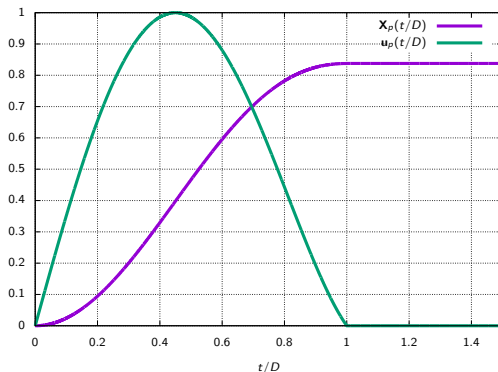
$$x^* = \frac{x}{L}, \mathbf{u}^* = \frac{\mathbf{u}}{U_\infty}, \mathbf{f}^* = \frac{\mathbf{f}L}{\rho_0 U_\infty^2}, \mathbf{F}^* = \frac{\mathbf{F}L}{\rho_1 U_\infty^2}$$

Doing so, several dimensionless parameters arises:

$$Re = \frac{U_\infty L}{\nu}, \quad Fr = \frac{gL}{U_\infty^2}, \quad \rho = \frac{\rho_1}{\rho_0 L}, \quad \gamma = \frac{K_b}{\rho_1 U_\infty^2 L^2}$$

## Plate imposed motion

We model isolated rotations using the analytical relationship proposed by Repetto et al. (2005).



- The angle is  $8^\circ$
- The maximum velocity is 0.061 m/s
- The duration is 0.045 s

## Parameters used in the computations

Quantity	Value	Reference
<b>Properties of the retinal flap</b>		
Density $\rho_S$	1300 kg/m <sup>3</sup>	
Length $L$	1.5 – 2.5 mm	
Thickness	70 $\mu$ m	Alamouti and Funk (2003), Foster et al. (2010), Ethier et al. (2004), Bowd et al. (2000), Wollensak and Eberhard (2004), Dogramaci and Williamson (2013)
Bending stiffness $K_b$	$2.98 \cdot 10^{-11}$ Nm <sup>2</sup>	$Eh^3/12$
Young's modulus $E$	$1.21 \cdot 10^3$ N/m <sup>2</sup>	Jones et al. (1992), Wollensak and Eberhard (2004), Reichenbach et al. (1991), Sigal et al. (2005)
<b>Properties of the fluid</b>		
Density $\rho_F$	1000 kg/m <sup>3</sup>	Foster et al. (2010)
Dynamic viscosity $\mu$	$1.065 \cdot 10^{-3}$ kg/ms	Foster et al. (2010)

**Table:** Parameter values used for the simulations and corresponding references when available.

# Dynamics for retinal tear

$$L=2 \text{ mm}, \theta = 33.6^\circ$$

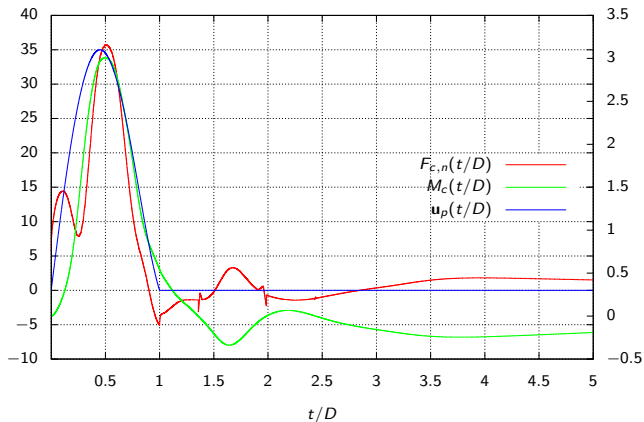
Movie 1

## Dynamics for retinal hole

$$L=2 \text{ mm}, \theta = 33.6^\circ, \Delta = 0.17 \text{ mm}$$

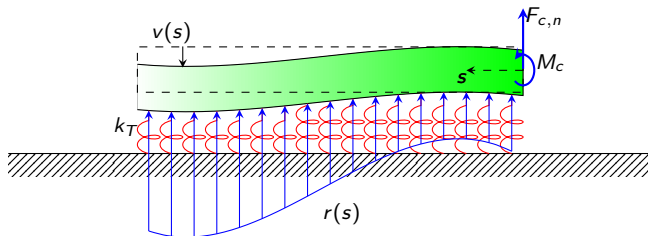
Movie 2

# Clamping force and torque evaluation



We evaluate the wall-normal force ( $F_{c,n}$ ) and torque ( $M_c$ ) at the clamping point as a function of time. These values are then used to model the **tendency to further detach**.

# Winkler theory



Semi-infinite foundation (in green) subject to a punctual force  $F_{c,n}$  and torque  $M_c$  at the finite end, and supported by elastic spring of stiffness  $k_T$  (in red). The soil reaction  $r(s)$  (in blue) is proportional to the foundation displacement  $v(s)$ .

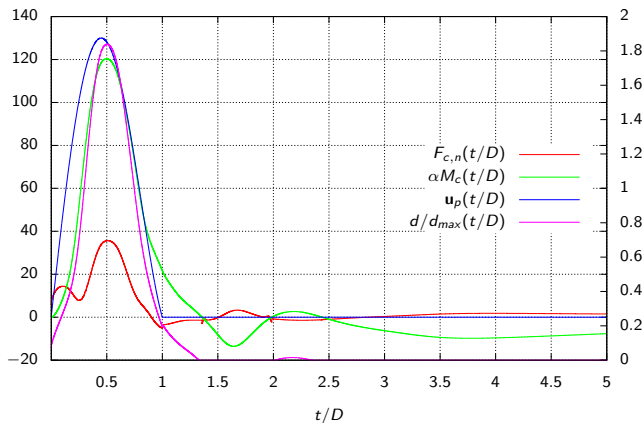
$$v(s) = \frac{e^{-\alpha s}}{2\alpha^3\gamma} \{ \alpha M_c [\cos(\alpha s) - \sin(\alpha s)] + F_{c,n} \cos(\alpha s) \},$$

$$d = \max(v|_{s=0}, 0) = \max\left(\frac{\alpha M_c + F_{c,n}}{2\alpha^3\gamma}, 0\right),$$

where  $\alpha$  is the ratio between the soil spring rigidity  $k_T$  and the foundation beam stiffness  $\gamma$ .

**$d$  is the tendency to detach**

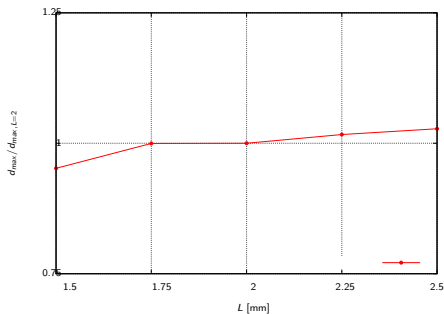
# Tendency to detach



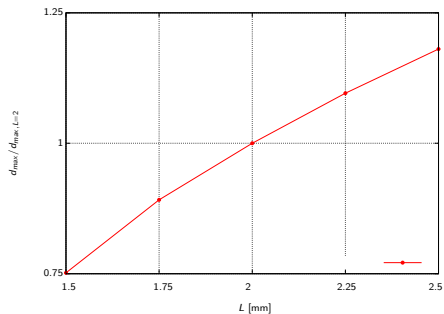
$d$  attains a maximum value for a finite value of  $t/D$

# Different filament lengths $L$ : maximum tendency to detach

clamping angle  $\theta = 33.56^\circ$ ,  $\Delta = 0.17\text{mm}$  (retinal hole)



Tear

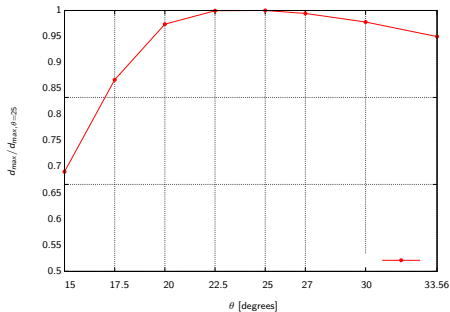


Hole

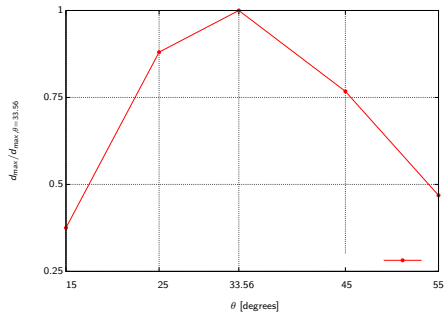
Increasing  $L$  increases the maximum value of  $d$

# Different clamping angles $\theta$ : maximum tendency to detach

length  $L = 2$  mm,  $\Delta = 0.17$  mm (retinal hole)



Tear

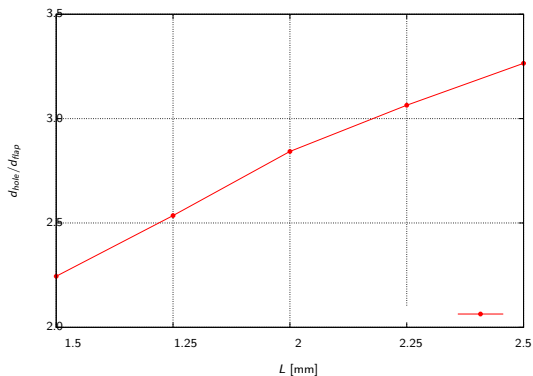


Hole

A maximum value of  $d$  is found

# Comparison horseshoe tear & hole: maximum tendency to detach

clamping angle  $\theta = 33.56^\circ$ ,  $\Delta = 0.17\text{mm}$  (retinal hole)



The retinal hole is more prone to detach compared to horseshoe tear

## Conclusions

The tendency to detach has been analyzed both for the **free flap** and **hole case** for different values of the detached retinal length, clamping angle and inter-tip distance (in the case of retinal hole). The general conclusions can be summarized as follows:

- The tendency to detach of a retinal hole, compared to a retinal free flap, is 2 - 3 times larger for retinal filaments of 1.5 - 2.5 mm, with increasing values of  $d$  for increasing values of the filament length.
- The tendency to detach increases as the retinal filament length increases, both for the retinal hole- and retinal free flap case.
- A worst-case angle is found when the tendency to detach is investigated for different clamping angles. The value is  $\simeq 25^\circ$  in the free flap case and  $\simeq 34^\circ$  in the hole case.
- The effect of changing the inter-tip distance, which is related to the size of the retinal hole, on the tendency to detach is weak.

## References I

- B. Alamouti and J. Funk. Retinal thickness decreases with age: an oct study. *British Journal of Ophthalmology*, 87(7):899–901, 2003.
- C. Bowd, R. N. Weinreb, B. Lee, A. Emdadi, and L. M. Zangwill. Optic disk topography after medical treatment to reduce intraocular pressure. *American Journal of Ophthalmology*, 130(3): 280 – 286, 2000. ISSN 0002-9394. doi: [http://dx.doi.org/10.1016/S0002-9394\(00\)00488-8](http://dx.doi.org/10.1016/S0002-9394(00)00488-8). URL <http://www.sciencedirect.com/science/article/pii/S0002939400004888>.
- M. Dogramaci and T. H. Williamson. Dynamics of epiretinal membrane removal off the retinal surface: a computer simulation project. *Br. J. Ophthalmol.*, 97 (9):1202–1207, 2013. doi: 10.1136/bjophthalmol-2013-303598.
- C. R. Ethier, M. Johnson, and J. Ruberti. Ocular biomechanics and biotransport. *Annu. Rev. Biomed. Eng.*, 6:249–273, 2004.
- W. J. Foster, N. Dowla, S. Y. Joshi, and M. Nikolaou. The fluid mechanics of scleral buckling surgery for the repair of retinal detachment. *Graefe's Archive for Clinical and Experimental Ophthalmology*, 248(1):31–36, 2010.
- I. L. Jones, M. Warner, and J. D. Stevens. Mathematical modelling of the elastic properties of retina: a determination of young's modulus. *Eye*, (6):556–559, 1992.
- B. Lee, M. Litt, and G. Buchsbaum. Rheology of the vitreous body. Part I: viscoelasticity of human vitreous. *Biorheology*, 29:521–533, 1992.

## References II

- C. S. Nickerson, J. Park, J. A. Kornfield, and H. Karageozian. Rheological properties of the vitreous and the role of hyaluronic acid. *Journal of Biomechanics*, 41(9):1840–6, 2008. doi: 10.1016/j.jbiomech.2008.04.015.
- A. Reichenbach, W. Eberhardt, R. Scheibe, C. Deich, B. Seifert, W. Reichelt, K. Dähnert, and M. Rödenbeck. Development of the rabbit retina. iv. tissue tensility and elasticity in dependence on topographic specializations. *Experimental Eye Research*, 53(2):241 – 251, 1991. ISSN 0014-4835. doi: [http://dx.doi.org/10.1016/0014-4835\(91\)90080-X](http://dx.doi.org/10.1016/0014-4835(91)90080-X). URL <http://www.sciencedirect.com/science/article/pii/001448359190080X>.
- R. Repetto, A. Stocchino, and C. Cafferata. Experimental investigation of vitreous humour motion within a human eye model. *Phys. Med. Biol.*, 50:4729–4743, 2005.
- I. A. Sigal, J. G. Flanagan, and C. R. Ethier. Factors influencing optic nerve head biomechanics. *Investigative Ophthalmology & Visual Science*, 46(11):4189, 2005. doi: 10.1167/iovs.05-0541. URL [+http://dx.doi.org/10.1167/iovs.05-0541](http://dx.doi.org/10.1167/iovs.05-0541).
- K. Swindle, P. Hamilton, and N. Ravi. In situ formation of hydrogels as vitreous substitutes: Viscoelastic comparison to porcine vitreous. *Journal of Biomedical Materials Research - Part A*, 87A(3):656–665, Dec. 2008. ISSN 1549-3296.
- G. Wollensak and S. Eberhard. Biomechanical characteristics of retina. *Retina*, (24):967–970, 2004.